Free Radical Biology & Medicine 50 (2011) 963–970

Contents lists available at ScienceDirect

Free Radical Biology & Medicine

journal homepage: www.elsevier.com/locate/freeradbiomed

Original Contribution

Changes in reactive oxygen species begin early during replicative aging of *Saccharomyces cerevisiae* cells

Yuen T. Lam, May T. Aung-Htut, Yu L. Lim, Hongyuan Yang, Ian W. Dawes *

School of Biotechnology and Biomolecular Sciences, University of New South Wales, Sydney, NSW 2052, Australia

ARTICLE INFO

Article history:
Received 27 July 2010
Revised 22 December 2010
Accepted 11 January 2011
Available online 19 January 2011

Keywords:
Reactive oxygen species
Superoxide anion
Yeast
Cell aging
Oxidative stress
Mitochondrial morphology
SIR2
Free radicals

ABSTRACT

Increased reactive oxygen species (ROS) are a feature of aging cells, but little is known about when ROS generation begins as cells age. Here we show how ROS change in *Saccharomyces cerevisiae* cells throughout their early replicative life span using the fluorescent ROS indicator dihydroethidium (DHE), which has some specificity for the superoxide anion. Cells in a particular age range were heterogeneous with respect to their ROS burden. Surprisingly, some cells as young as 5–7 generations acquired a greatly increased level of ROS detected by DHE relative to virgin cells. By 12 generations 50% of cells had a substantial ROS burden despite being only halfway through their life span. In contrast to the wild type, cells of a *sir2* mutant had lower levels of ROS reacting with DHE. Daughters from older mothers had low ROS levels, and this asymmetric distribution of ROS was *SIR2*-independent. Mitochondrial fragmentation also began to occur in cells after 4 generations and increased markedly as cells aged. Daughter cells regenerated normal tubular mitochondria despite the fragmentation of mitochondria in the mother cells, whereas daughters of the *sir2* mutant had fragmented mitochondria at all ages.

Aerobic organisms utilize oxygen as the electron acceptor for the electron transport chain [1]. However, approximately 5% of electrons leak from the electron transport chain, generating reactive oxygen species (ROS) including the superoxide anion ($O_2^{\bullet-}$) and hydrogen peroxide (H_2O_2) [2,3], which can cause oxidative damage to DNA, proteins, and lipids [4,5]. Harman [6] first proposed the Free Radical Theory of Aging, which states that ROS produced during aerobic metabolism cause accumulated irreversible cellular damage leading to cell senescence and death.

This theory received considerable support from studies of a wide range of model organisms such as *Drosophila melanogaster*, *Caenorhabditis elegans*, and *Saccharomyces cerevisiae*, which showed a strong correlation between increased levels of ROS and oxidatively damaged molecules as cells aged [7,8]. Tissues from patients with age-related diseases, including premature aging diseases, have increased levels of oxidatively damaged (carbonylated) proteins compared to those from age-matched healthy individuals [9]. In some organisms, overexpression of genes encoding antioxidant enzymes increases longevity [10–12], and some of the longevity genes of *C. elegans* play a role in detoxification of oxygen radicals [13,14]. Despite this, there are conflicting outcomes of studies to determine whether oxidative damage to cellular constituents or the life span of an organism is correlated with changes in antioxidant defense mechanisms [15] and research is still ongoing to determine if ROS trigger or accelerate aging.

The yeast *S. cerevisiae* has provided a model for aging studies because it undergoes a process of "mother cell-specific" aging (replicative aging) in which the probability of senescence of a mother cell increases exponentially with age [16–18]. As the cells age they become sterile and eventually die [19]. The replicative life span of these cells is the number of generations an individual mother cell undergoes before reaching senescence and ceasing to divide [20]. There is a clear relationship of this aging process to that of higher organisms with a number of important similarities [21,22]. These include phenotypic similarity of the aged cells and the fact that activated *RAS* alleles decrease life span [23–25]. Deletion of the yeast *SGS1* gene (homologue of the *WRN* gene mutated in the premature aging disease Werner syndrome) leads to a reduction in cellular life span [26]. The *S. cerevisiae SIR2* gene, encoding the NAD^+-dependent histone deacetylase Sir2p, is involved in life-span extension, and its function is also highly conserved in eukaryotes [27,28]. In *S. cerevisiae*, ROS are very high in old cells but not in their daughter cells [29,30] and this asymmetrical distribution of ROS is reported to depend on Sir2p [30].

There is indirect evidence from heterogeneity of yeast cell populations that ROS production may occur relatively early in the life span of the organism [31] but it is not clear when during the life span these ROS levels began to increase. Although there is evidence that an increased level of ROS contributes to cell aging, and that oxidatively damaged species such as carbonylated proteins accumulate as cells age [32], it is still not clear whether ROS gradually increase during the lifetime of a cell

Abbreviations: ROS, reactive oxygen species; GFP, green fluorescent protein; WGA, wheat germ agglutinin; DHE, dihydroethidium bromide; PI, propidium iodide.

* Corresponding author. Fax: +61 2 93851050.
E-mail address: i.dawes@unsw.edu.au (I.W. Dawes).

0891-5849/$ – see front matter © 2011 Elsevier Inc. All rights reserved.
doi:10.1016/j.freeradbiomed.2011.01.013

or there is a sudden burst of ROS at the later stages that leads to senescence and death. Therefore, we determined the level of ROS in cells of different ages in *S. cerevisiae*. We also analyzed changes throughout the replicative life span in morphology of mitochondria, because these are major sites of ROS production in cells.

Materials and methods

Growth conditions and media

S. cerevisiae diploid strain BY4743 (*MAT***a**/*MATα; his3Δ1/his3Δ1; leu2Δ0/leu2Δ0; met15Δ0/MET15; LYS2/lys2Δ0; ura3Δ0/ura3Δ0*) and its isogenic *sir2/sir2* and *sod1/sod1* mutants were used. Cells were grown at 30 °C with aeration in SC medium with the concentrations of amino acids/bases used according to [33]. For visualization of mitochondria, cells were transformed with the pUC35–aconitase (*ACO1*)–GFP fusion construct [34] and grown in medium lacking uracil.

Isolation of replicative-age mother cells

Replicative-age mother cells were isolated by the biotin–magnetic sorting procedure [35]. Cells grown in 10 ml SC medium to OD_{600} 0.3–0.4 were washed three times with sterile PBS and labeled with sulfo-NHS-LC-biotin (Pierce Protein Research Products, Rockford, IL, USA) for 30 min at room temperature. Cells were then washed three times with PBS containing 100 mM glycine to remove unbound biotin. The biotinylated cells were reinoculated into fresh SC medium to allow the cells to divide. The first enrichment round (R_1M) was collected 2 h after reinoculation. The second enrichment round (R_2M) was collected 12 h after reinoculation of the R_1M cell population in fresh medium and the third enrichment round (R_3M) 12 h after reinoculation of the R_2M cell population. All cultures were maintained at OD_{600} <2 to prevent the cells from entering stationary phase. Cells collected at each enrichment step were washed three times with degassed buffer (PBS, pH 7.2, 0.5% bovine serum albumin, 2 mM EDTA) and incubated with anti-biotin microbeads (Miltenyi Biotec, Sydney, Australia) for 15 min at 4 °C. The cells were then washed three times with degassed buffer and loaded onto a magnetic column (Miltenyi Biotec) prewetted with degassed buffer. Newly produced daughter cells were collected as an eluate from the magnetic column. Biotin-labeled mother cells were obtained by removing the column from the magnet and flushing the column with 1 ml of degassed buffer. The percentages of daughter and mother cells in sorted cell populations were determined by counting the number of bud scars on their cell surface after staining as described below.

Wheat germ agglutinin, dihydroethidium bromide, and propidium iodide staining

Bud scars were counted using Alexa Fluor 633-conjugated WGA (Molecular Probes, Sydney, Australia), which selectively bind to chitinous bud scars. Cells were washed with PBS and stained with WGA (50 μg/ml final concentration) at 30 °C for 30 min in the dark. The fluorescent probe DHE (Molecular Probes) was used to determine levels of ROS. DHE was added to cells at a final concentration of 5 μg/ml and incubated at 30 °C for 5 min. Cell viability was determined by adding PI (Sigma, Sydney, Australia) at a final concentration of 3 μg/ml and incubating at room temperature for 5 min.

Flow cytometric analysis

FACS analysis was performed using a FACSAria (BD Biosciences, Sydney, Australia). For sorting PI-unstained cells, a gate was defined around a single population of unstained cells within a bivariate dot plot of forward scatter and PE-A (excitation 488, emission 585/42). Events detected within the gate were sorted as a PI-negative population and those detected outside the gate were sorted as a PI-stained population. Cells were sorted directly into FACS tubes for further staining and analysis. Data were analyzed from four independent biological replicates using FlowJo software (TreeStar, Inc., Ashland, OR, USA).

Microscopic examination

Cells were examined using a fluorescence microscope (BX60 Olympus/LEICA DM5500B) under a 100× objective. The morphology of mitochondria was visualized by GFP fluorescence and the number of bud scars was counted after staining with WGA. The micrographs taken were representative of the morphology of the cells.

Results

The age distributions of isolated mother and daughter populations

In an exponentially growing culture, aged cells are of low abundance, and it is important to enrich an aged cell population before performing analyses. Of several methods available to separate old and young yeast cells [29,36–38] we chose the biotin labeling–magnetic sorting technique [35], which relies on the fact that biotinylated cell wall is retained on the surface of mother cells and not passed on to newly generated daughter cells.

Cells of exponentially grown wild-type and Δ*sir2* mutant cultures were labeled with biotin and reinoculated into fresh SC medium to allow further cell division before enrichment of the biotin-labeled cells using magnetic sorting. Isolated biotin-labeled cells represent mothers and the non-biotin-labeled newly produced progeny were daughters. A portion of the mother cell fraction was reinoculated in fresh medium for 12 h further growth and reisolated. The isolation of mother and daughter cells was repeated three times for the wild type but only twice for the Δ*sir2* mutant because of incomplete segregation between mother and daughter Δ*sir2* cells during the third separation. The age of both mother and daughter cells isolated from each round of sorting was determined by staining bud scars with Alexa Fluor-633-conjugated WGA [39] and counting them using fluorescence microscopy. The distribution of cell age within the population was also determined by flow cytometry measuring the fluorescence intensity.

A progressive increase in age, as indicated by increasing number of bud scars, was observed in both the wild-type (Fig. 1A) and the Δ*sir2* (Supplementary Fig. 1A) mother populations (M) with each enrichment. Approximately 80% of mother cells had undergone 1–3 generations after the first enrichment (R_1M). The second enrichment (R_2M) resulted in 71% of mother cells of 6–9 generations, and about half of the mother cells were 10–13 generations old after the third enrichment (R_3M). On the other hand, the age distributions of daughter cells (D) collected from each round of the enrichment remained similar (age 0–3). Approximately 70% of isolated daughter cells from the first selection (R_1D) were virgin cells with a single stretched birth scar. The majority of daughter cells isolated from the second (R_2D) and third enrichments (R_3D) were 1–3 generations old (approximately 83 and 90% of the population, respectively). Similar results were obtained for the Δ*sir2* mutant for the first and second rounds of enrichment.

The fluorescence intensity of wild-type and Δ*sir2* mother cells stained with WGA also increased with each separation round as determined by FACS (Fig. 1B for the wild type; Supplementary Fig. 1B for Δ*sir2*). To verify that the increase in fluorescence intensity observed by FACS was related to cell age (increased number of bud scars), we collected cells in four sets according to the intensity of WGA signal, as shown in Fig. 2, and estimated the average number of bud scars in individual subpopulations. Cells with 0–4 bud scars were found in the set with fluorescence intensities below 10^1 (G1) and those with 5–9 and 7–12 bud scars were found in the populations with fluorescence intensity 10^1–10^2 (G2) and 10^2–10^3 (G3), respectively. Because the magnetic sorting approach was effective in enriching cell populations

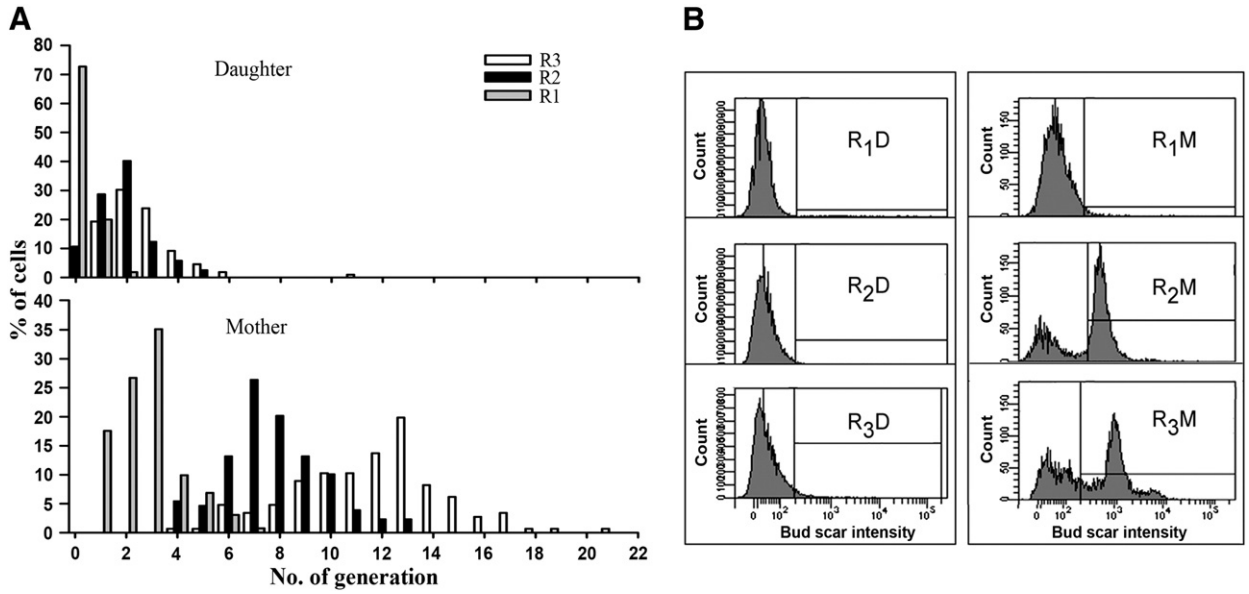

Fig. 1. The distribution of bud scars in wild-type mother (M) and daughter (D) cells isolated using the biotin–magnetic sorting procedure. Progressively aged mother cells were isolated from their daughter cells in three rounds (R_1–R_3) as described under Materials and methods. Bud scars of the isolated populations were stained with WGA and the number of bud scars was (A) counted by fluorescence microscopy and (B) analyzed by flow cytometry.

according to age, we therefore analyzed ROS production in both mother (R_nM) and daughter (R_nD) populations.

ROS level changes begin in relatively young cells

To determine when cells begin to have increased ROS levels as they age, ROS levels were estimated in cells isolated from three sequential enrichments composed of progressively aged cells. Each set of separations was repeated on four separate occasions and the fluorescent probe DHE, which has specificity toward $O_2^{\bullet-}$, was used to detect ROS production. In addition, cells were stained with the bud scar stain WGA to determine the age of each individual cell and PI to assess membrane leakage, which is indicative of cell death. All stained cells were then analyzed by FACS.

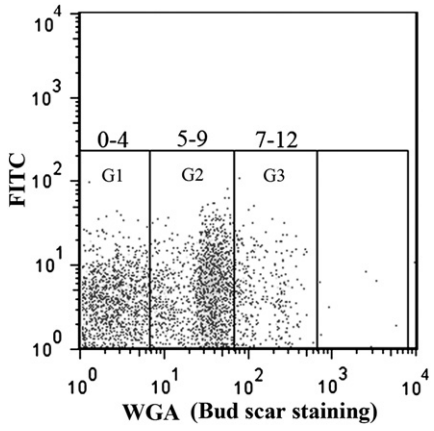

Fig. 2. The relationship between cell age and fluorescence intensity of WGA-stained cells. Exponentially grown wild-type cells were stained with bud scar stain WGA and sorted and collected according to fluorescence intensity as shown (G1–G3). The average number of bud scars was counted using a fluorescence microscope for each population (G1–G3) as indicated.

Data for a representative experiment are shown in Fig. 3A. There was an increase in ethidium fluorescence beginning at round 2 when cells had had an average age of six to nine divisions. From this it appeared that ROS increase markedly in cells early in the aging process, although several points needed to be resolved before this could be concluded. First, in different separations there was variability in the age of cells obtained at each round of enrichment (Supplementary Fig. 2), which hindered statistical analysis. Second, the proportion of PI-stained cells in the population increased as the cells progressively aged (Fig. 3A). Although aging cells die naturally, some PI staining may have been due to physical stress during magnetic sorting leading to cell leakage. This is less likely because the increase in PI staining seen in separated cells was far more severe in mothers than in daughters despite both having gone through the same enrichment procedure (Table 1). The percentage of mother cells stained with PI increased from around 1% in round 1 to 26% in round 3 of enrichment, whereas in daughter cells, there was less than 2% stained even at the end of round 3. A similar increase in PI-stained cells was also observed for Δ*sir2* mother cells (Supplementary Table 1). However, there remains the possibility that magnetic separation procedures used in this study had differential effects on mother and daughter cells because of differences in cell size and possible sensitivity to physical stress. Some PI-stained cells may also be DHE-positive, which would make it difficult to determine for older cells whether an increase in DHE fluorescence was due to cell death or to an increase in $O_2^{\bullet-}$. It was not possible to costain with both PI and DHE because their emission spectra overlap.

To resolve these issues, the above experiments were repeated four times but with PI-stained cells being discarded before staining the remaining live cells with DHE. The discarded PI-stained cells had, as expected, already undergone a substantial number of cell divisions (Supplementary Fig. 3). The PI-negative cells were retested with PI to ensure that they represented the PI-negative population and an aliquot was taken for ROS analysis. The results of DHE staining after PI-positive cells were removed are shown in Fig. 3B.

To avoid variability caused by differences in age distribution of cells from different selection rounds, changes in the percentage of DHE-positive cells were compared for cells in discrete age ranges using

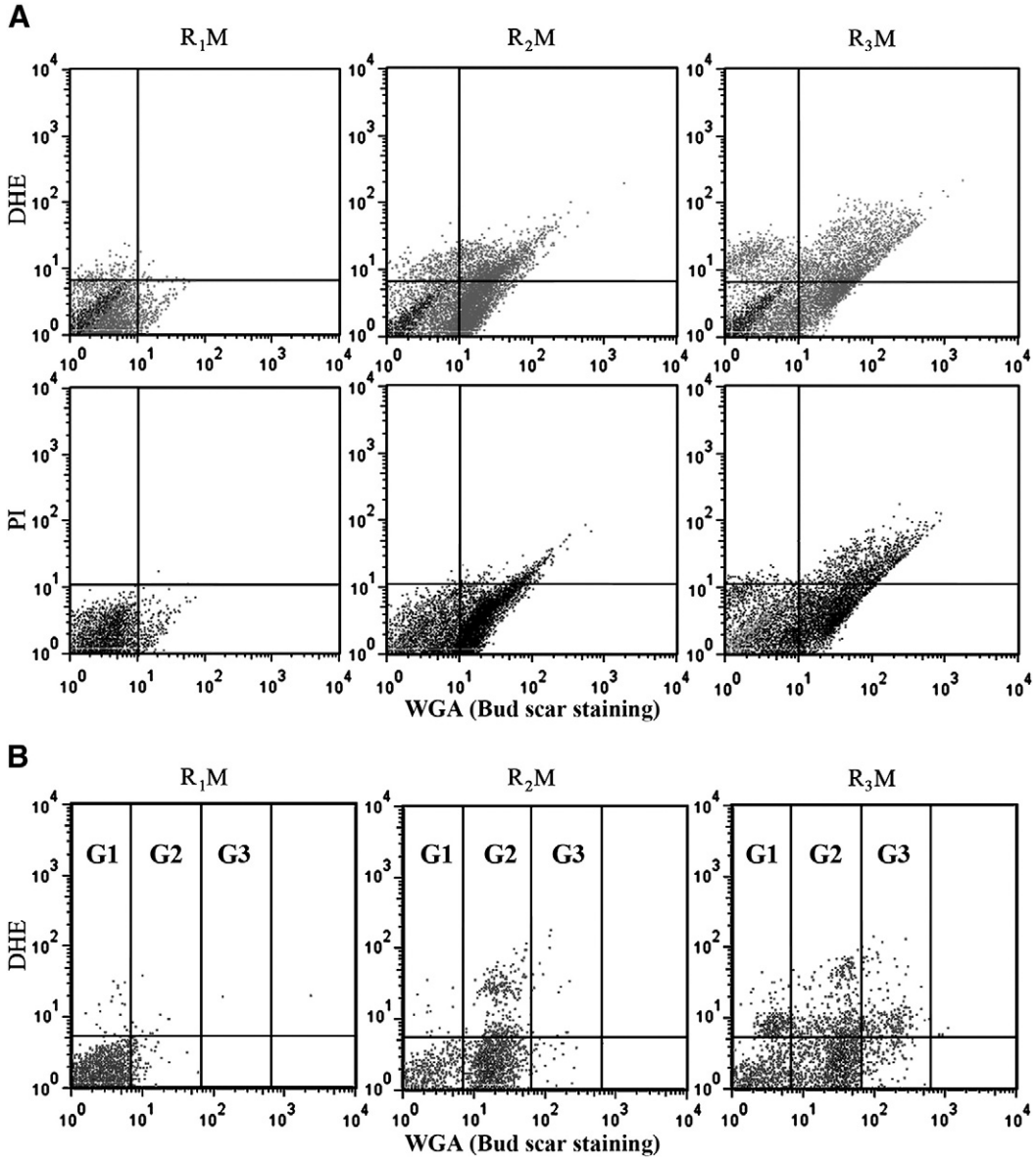

Fig. 3. Determination of $O_2^{\bullet-}$ level and PI-permeable cells in progressively aged cells. (A) Aging mother populations isolated from three rounds of selection (R_1M–R_3M) were separately stained with DHE (for $O_2^{\bullet-}$) and PI (for cell death) and the bud scars were also stained with WGA. Increase in fluorescence intensity of DHE and PI was compared to the negative control cells with no staining and the dot plots were separated into four quadrants based on unstained control cells. (B) The level of $O_2^{\bullet-}$ in cells isolated from R_1M–R_3M after excluding PI-positive cells was analyzed by staining with DHE. The number of generations was determined by staining bud scars with WGA. The DHE-positive (top) and -negative (bottom) cells are divided by the horizontal line and vertical lines separate cells by age range according to Fig. 2.

subpopulations, G1–G3, based on bud scars as shown in Fig. 2. The analysis was performed by comparing the percentage of cells stained with DHE (i) among mother cell populations, (ii) between mother and daughter cell populations, and (iii) between the wild type and the Δ*sir2* mutant. Data are shown in Fig. 4 and were analyzed using a two-tailed *t* test, and *p* values ≤ 0.1 were regarded as significant.

Cells of the same age range showed a similar percentage of DHE-positive cells even when they were isolated from different enrichment rounds or biological replicates. In the wild type, 3.3% of the G1 subpopulation (age 0–4) were DHE-positive (Fig. 4A). DHE-positive wild-type cells increased to 21.9% in the G2 subpopulation (age 5–9) and 46.4% in the G3 cells (age 7–12) (Fig. 4A). The data in Figs. 3 and 4A show that cells in a particular age range are heterogeneous with respect to their superoxide burden and that there is a chance that even cells as young as seven generations will have acquired a greatly increased level of $O_2^{\bullet-}$ relative to virgin cells. Moreover, the maximum DHE fluorescence seen in individual cells increased further as cells aged (Fig. 3, from G1 to G2).

Surprisingly, young cells of the Δ*sir2* mutant had fewer DHE-positive cells than the wild type (G1; age 0–4; Fig. 4A). As the mutant cells aged, the percentage of DHE-positive cells increased from 2.1% in G1 cells (age 0–4) to 17.5 and 24.5% in G2 (age 5–9) and G3 subpopulations (age 7–12).

Table 1
The percentage of wild-type cells stained with PI after each round of enrichment

	Mother (%)	Daughter (%)
Round 1	1.2 (1.3)	0.2 (0.1)
Round 2	6.4 (2.1)	0.5 (0.5)
Round 3	26.7 (14.6)	1.6 (1.0)

The averages and (SD) of four biological replicates are shown.

The distribution of ROS between mothers and their progeny

Our data confirm the previous finding that mother cells have a higher level of ROS than their daughters [29]. This means that either ROS are distributed unequally between mother and daughter cells or

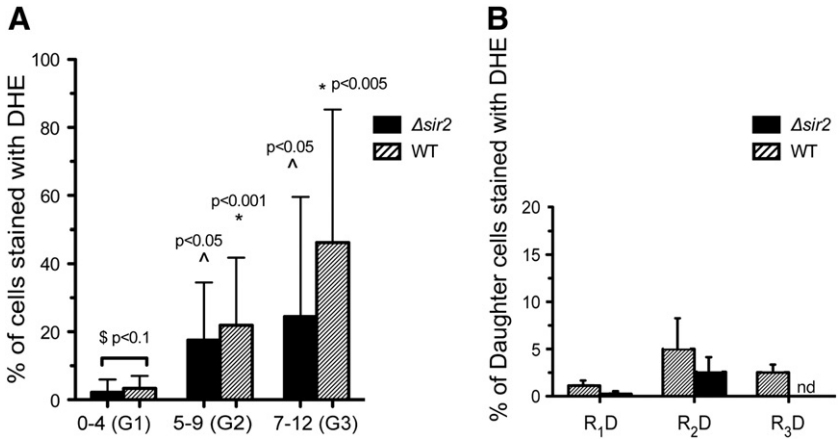

Fig. 4. ROS in old and young wild-type (WT) and Δ*sir2* mutant cells. Mother and daughter WT and Δ*sir2* cells were isolated from three (R_1–R_3) and two (R_1 and R_2) rounds of enrichment, respectively, as described under Materials and methods. Cells were stained with WGA and DHE and analyzed by flow cytometry. (A) The percentage of cells stained with DHE was analyzed for cells with similar age intervals (G1–G3, as in Fig. 2) generated from the three enrichments. (B) Percentages of both WT and Δ*sir2* daughter cells stained with DHE were also determined for two or three enrichment rounds (R_1D–R_3D); nd, not done. The analysis was performed on four biological replicates from independent experiments. The Student *t* test was used to determine *p* values. $Wild type vs Δ*sir2;* *WT G2/G3 vs G1; ^Δ*sir2* G2/G3 vs G1.

that the daughter cells are efficient in removing ROS. Erjavec and Nystrom [30] analyzed the levels of ROS in old mothers and daughters before and after cytokinesis and showed that unequal partitioning of ROS occurred only after cytokinesis and that *SIR2*-dependent protein segregation is responsible for this asymmetry. However, the ROS distribution between the mother cells and their progeny at specific ages has not been determined. Therefore we examined the level of ROS in daughter cells produced from mothers in different age ranges isolated from three rounds of enrichment. If there is asymmetrical ROS distribution, daughter cells generated from mothers at different ages should have similar and lower levels of ROS compared to mothers. On the other hand, if the distribution of ROS is symmetrical, increasing levels of ROS should be observed in daughter cells produced from progressively aged mothers.

The average number of both wild-type and Δ*sir2* mutant (Fig. 4B) cells stained with DHE varied among the daughter populations (R_1D–R_3D) generated from mothers with increasing number of generations. However, the percentage of DHE-positive cells found in the daughter populations did not differ significantly from one another for both the wild-type and the Δ*sir2* mutant cells and did not increase with age of their mothers. Asymmetrical distribution of ROS was therefore observed regardless of the mother age (up to 12 generations). Notably this was also the case in the absence of *SIR2,* which does have a role in the asymmetrical distribution of carbonylated proteins [32].

Mitochondrial morphology changes early during replicative aging

Because mitochondria are major sites of $O_2^{\bullet-}$ production and elevated levels of ROS can damage mitochondria, we monitored changes in mitochondrial morphology as cells aged. Cells overexpressing the fusion protein *ACO1*–GFP were subjected to magnetic separation as before and their mitochondrial morphology was visualized via GFP. The use of this construct has been validated [34]. Mitochondria of wild-type cells underwent marked changes in morphology as cells aged (Fig. 5A). Initially in the R_1M population (age 3–4) mitochondria were elongated tubules with (~25%) and without (~75%) partial fragmentation. This morphology continuously changed and in the R_2M population (age 8–10) mitochondria with either highly branched (~40%) or fragmented structures (~60%) were observed. The mitochondria were severely fragmented with no tubular structure (~80%) in the R_3M population (age 11–13). Similar changes in mitochondrial morphology were observed when the MitoTracker DeepRed fluorescence probe was used to visualize mitochondria (Supplementary Fig. 4). These results indicated that mitochondria fragment early during replicative aging.

Daughter cells obtained after each enrichment had tubular mitochondria although some cells displayed partial fragmentation (~20%) after R_3D. Because mitochondria are not formed de novo and daughter cells are derived from mother cells, the R_3D daughter cells should have inherited fragmented mitochondria from mother cells in which nearly 80% had fragmented mitochondria. Because the majority of R_3D daughter cells had tubular mitochondria it is clear that daughter cells can regenerate tubular structures despite the presence of fragmented structures in their mothers. There was some fragmentation in the daughters of older mother cells and these data confirm the conclusions of Lai et al. that in mother cells mitochondria become dysfunctional with age and that older mothers have an increased tendency to segregate dysfunctional mitochondria to their daughters [40].

Interestingly, mitochondria of Δ*sir2* cells were fragmented severely even in cells of one to three generations (~80% of cells) and the fragmented structures persisted in older cells (Fig. 5B). Moreover, newly produced Δ*sir2* daughter cells at each round of selection also displayed fragmented mitochondria. Deletion of *SIR2* may impose stress, and mitochondrial fragmentation may be an indication of cellular stress and not specific to deletion of *SIR2*.

Because ROS readily attack mitochondria, to determine whether the ability of daughters to recover from the fragmented mitochondria is limited by high intracellular ROS levels, we investigated the mitochondrial morphology of the Δ*sod1* mutant, which has high levels of free radicals, including $O_2^{\bullet-}$ [41,42]. Interestingly, mitochondria in young cells of the Δ*sod1* strain were tubular (Fig. 6). This indicated that the ability of young cells to maintain or regenerate tubular mitochondria was not greatly affected in cells having elevated intracellular levels of $O_2^{\bullet-}$.

Discussion

Although ROS levels are known to be very high in aged cells [29], it is surprising that a dramatic elevation of ROS levels can occur in yeast cells between 5 and 9 generations, which is not yet one-third of their mean replicative life span (28 generations in the wild-type BY4743; Supplementary Fig. 5), and the proportion of cells with higher levels of ROS increases as cells age. By the time the cells approach middle age, around 50% have high levels of ROS, yet only about 10% of the population will cease to divide in the next 5 generations. Even if those cells that acquire high levels of ROS die sooner, it is clear that most can survive for many more generations after the change in ROS level.

These results indicate that it might be possible to test aspects of the free radical theory of aging by exploiting the heterogeneity (with respect to ROS levels) of cells of the same age. This might be achieved

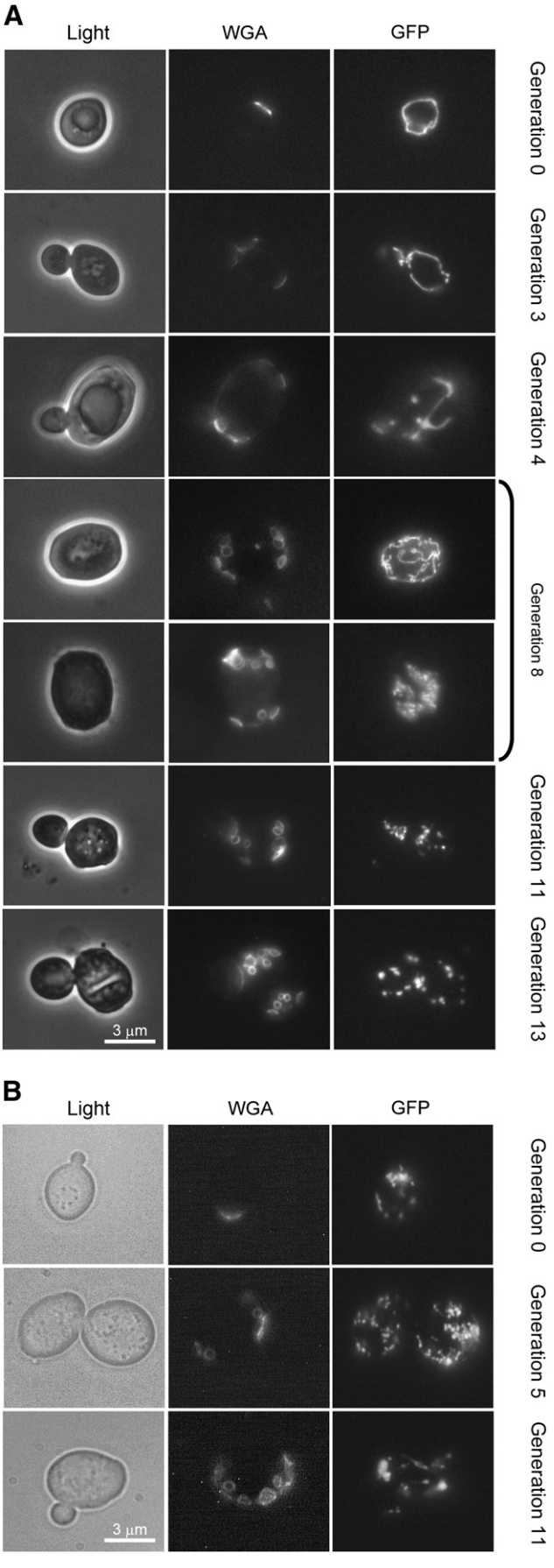

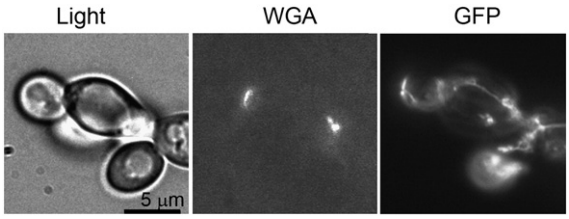

Fig. 6. Mitochondrial morphology of young Δ*sod1* mutant cells. Cells carrying the *ACO1*–GFP construct were stained with bud scar stain WGA and those with only one bud scar were assessed by fluorescence microscopy for their mitochondrial morphology.

by sorting cells of defined age that have an increased burden of ROS, using FACS, and subsequently testing whether they have a reduced life span compared to those cells of the same age but with low ROS levels. We have, therefore, analyzed subpopulations of cells with different levels of DHE staining using FACS sorting. Unfortunately, after FACS of DHE-stained cells, approximately 35% of DHE-positive cells and 60% of DHE-negative cells were respiratory-deficient petites (Supplementary Fig. 6), presumably as the result of exposure of the mitochondrial genome to ethidium, which is known to induce petite formation in yeast at high frequency. The petite mutation affects life span in a variable way dependent on strain [40,43,44]; hence the presence of a high level of petites in the population after sorting abrogates the usefulness of this approach based on FACS sorting. Although it is not possible to draw a firm conclusion concerning the direct role of ROS in aging, it is clear from the data that ROS levels increase markedly in some young cells and continue to increase throughout the aging process instead of suddenly increasing at the end of a cell's life span.

It is intriguing that cells can maintain their replicative potential and survive until their destined life span despite a constant increase in ROS. This survival may be due to the action of cellular antioxidant defense and repair mechanisms [4]. The increasing level of ROS in aged cells indicates that the antioxidant defense systems are not efficient enough to maintain a low level of ROS or that they are eventually damaged by ROS and became inefficient. The latter possibility is supported by the fact that a decrease in superoxide dismutase activity has been observed in replicatively aged cells [45]. Moreover, it is known that the activity of other key antioxidants also diminishes with aging; catalase activity is reduced and there is an increase in oxidized glutathione in old mothers [45].

We also observed heterogeneity with regard to ROS levels in cells of the same age range in the population, as was hinted at previously [31]. Depending on their level of oxidative stress and antioxidant capacity, cells might exceed a "redox threshold" at different ages. Even in a controlled environment such as continuous culture, cells oscillate between oxidative and reduced states as measured by the levels of glutathione and NAD(P)H [46], and therefore it is likely that cells with different redox states can exist in batch culture. Inevitably, cells are prone to shift to a more oxidized state as they age. This heterogeneity of oxidative stress within an aging population may partly contribute to the stochastic nature of cell aging seen in the distribution of ages at which cells cease to divide.

This elevation of oxidative stress during aging is largely due to an increased level of $O_2^{\bullet-}$, rather than of peroxides. $O_2^{\bullet-}$ is also important for cell signaling [47], because it can activate a number of protein kinases. Hence, although $O_2^{\bullet-}$ generated in young cells may be involved in normal biological processes, it also leads to the generation of hydrogen peroxide and very reactive hydroxyl radicals through the Fenton reaction [48,49], which would increase the cellular level of

Fig. 5. Changes in mitochondrial morphology of the (A) wild-type and (B) Δ*sir2* mutant cells during replicative aging. Progressively aged cells carrying the *ACO1*–GFP construct were isolated from various rounds of enrichment. The age of the isolated cells was determined by WGA staining and representative images of their mitochondrial morphology are shown.

oxidative stress and eventually decrease life span through the accumulation of damage caused by the ROS.

Surprisingly, we observed that cells of the short-lived Δ*sir2* mutant had less $O_2^{\bullet-}$ than the wild-type strain—especially young cells. Previous studies have shown that a higher level of $O_2^{\bullet-}$ was detected in the Δ*sir2* mutant [30]; the difference may be due to our excluding PI-positive cells. Levels of ROS detected in daughter cells generated from mothers with ages ranging from 1 to 12 generations did not support the proposal that asymmetrical distribution of ROS between mothers and daughters is dependent on *SIR2* [30]. ROS were unequally distributed between mothers and daughters in the absence of *SIR2*, with only a slight increase in ROS levels in the Δ*sir2* daughters from older mothers. Daughters isolated from mother cells (aged up to about 12 generations) seem to have a *SIR2*-independent mechanism for removal of ROS that differs from the mechanism for removing ROS-damaged cellular components, such as carbonylated proteins, which requires participation of *SIR2* and actin filaments in retaining damaged protein in mother cells [50].

Because mitochondria are the major sites of ROS production, they are prone to ROS attack, and we observed an early mitochondrial fragmentation in replicatively aged *S. cerevisiae*. Although wild-type daughter cells inherit mitochondria from among those that are fragmented in mother cells, they can regenerate them into the elongated tubular structures. This is another example of the asymmetry between mother and daughter cells during replicative aging of *S. cerevisiae*. Proper segregation of mitochondria is critical for daughter cells to acquire a full potential life span during cell replicative aging, and the Δ*atp2* mutant, which shows a defect in segregating functional mitochondria to daughter cells, has a reduced life span [40]. Our results show that most daughter cells produced by the mother cells up to 13 generations old readily regenerate mitochondria with a tubular structure. It remains to be determined when daughter cells begin to lose their ability to regenerate mitochondria.

SIR2 is involved in the regulation of an asymmetrical distribution of carbonylated protein between mother and daughter cells [30,32]. In the Δ*sir2* mutant, mitochondria fragmented much earlier than in the wild-type cells (80% fragmentation in cells of 1–3 generations) and fragmented mitochondria were found even in virgin cells. It is therefore possible that *SIR2* regulates other factors that are essential in the maintenance of mitochondrial morphology. It should be noted that the median life span for the Δ*sir2* mutant was 10 generations (Supplementary Fig. 5) and because most of the cells have fragmented mitochondria within a few generations, cells with fragmented mitochondria can survive on average of around 10 generations. So the onset of mitochondrial fragmentation need not lead to immediate senescence in the wild type, but may contribute to earlier cell loss of replicative potential. It is also important to note that the Δ*sod1* mutant had an even shorter life span than the Δ*sir2* mutant (Supplementary Fig. 5). If this reduction is due to the higher rate of superoxide production, then ROS-induced damage would seem to be much more relevant to aging than mitochondrial fragmentation.

In this study, we have shown that a burst of ROS occurs in cells at a relatively young age relative to senescence and ROS continue to increase in level throughout their lifetime. We also show that *SIR2* may play a role in maintenance and/or regeneration of mitochondrial integrity during aging. We also propose that there is a *SIR2*-independent regulatory mechanism for maintaining the asymmetrical distribution of ROS between presenescent mother cells (up to 12 generations) and their daughters.

Acknowledgments

This work was supported by the Australian Research Council. Y.T.L. was supported by an Australian Postgraduate Award from the Australian Research Council. We are grateful to Saskia Graf for technical assistance and Gabriel Perrone and Geoff Kornfeld for constructive comments.

Appendix A. Supplementary data

Supplementary data to this article can be found online at doi:10.1016/j.freeradbiomed.2011.01.013.

References

[1] Hatefi, Y. The mitochondrial electron transport and oxidative phosphorylation system. *Annu. Rev. Biochem.* **54:**1015–1069; 1985.
[2] Bouveris, A.; Cadenas, E. Production of superoxide radicals and hydrogen peroxide in mitochondria. In: Oberley, L.W. (Ed.), Superoxide Dismutases. CRC Press, Boca Raton, FL,pp. 15–30; 1982.
[3] Boveris, A. Determination of the production of superoxide radicals and hydrogen peroxide in mitochondria. *Meth. Enzymol.* **105:**429–435; 1984.
[4] Temple, M. D.; Perrone, G. G.; Dawes, I. W. Complex cellular responses to reactive oxygen species. *Trends Cell Biol.* **15:**319–326; 2005.
[5] Perrone, G. G.; Tan, S. X.; Dawes, I. W. Reactive oxygen species and yeast apoptosis. *Biochim. Biophys. Acta* **1783:**1354–1368; 2008.
[6] Harman, D. Aging: a theory based on free radical and radiation chemistry. *J. Gerontol.* **11:**298–300; 1956.
[7] Muller, F. L.; Lustgarten, M. S.; Jang, Y.; Richardson, A.; Van Remmen, H. Trends in oxidative aging theories. *Free Radic. Biol. Med.* **43:**477–503; 2007.
[8] Bokov, A.; Chaudhuri, A.; Richardson, A. The role of oxidative damage and stress in aging. *Mech. Ageing Dev.* **125:**811–826; 2004.
[9] Stadtman, E. R. Protein oxidation and aging. *Science* **257:**1220–1224; 1992.
[10] Sohal, R. S.; Weindruch, R. Oxidative stress, caloric restriction, and aging. *Science* **273:**59–63; 1996.
[11] Melov, S.; Ravenscroft, J.; Malik, S.; Gill, M. S.; Walker, D. W.; Clayton, P. E.; Wallace, D. C.; Malfroy, B.; Doctrow, S. R.; Lithgow, G. J. Extension of life-span with superoxide dismutase/catalase mimetics. *Science* **289:**1567–1569; 2000.
[12] Finch, C. E.; Ruvkun, G. The genetics of aging. *Annu. Rev. Genomics Hum. Genet.* **2:** 435–462; 2001.
[13] Gems, D. Nematode ageing: putting metabolic theories to the test. *Curr. Biol.* **9:** 614–616; 1999.
[14] Taub, J.; Lau, J. F.; Ma, C.; Hahn, J. H.; Hoque, R.; Rothblatt, J.; Chalfie, M. A cytosolic catalase is needed to extend adult lifespan in *C. elegans daf-C* and *clk-1* mutants. *Nature* **399:**162–166; 1999.
[15] Aguilaniu, H.; Gustafsson, L.; Rigoulet, M.; Nystrom, T. Protein oxidation in G0 cells of *Saccharomyces cerevisiae* depends on the state rather than rate of respiration and is enhanced in *pos9* but not *yap1* mutants. *J. Biol. Chem.* **276:** 35396–35404; 2001.
[16] Jazwinski, S. M. Growing old: metabolic control and yeast aging. *Annu. Rev. Microbiol.* **56:**769–792; 2002.
[17] Jazwinski, S. M. Longevity, genes, and aging. *Science* **273:**54–59; 1996.
[18] Pohley, H. J. A formal mortality analysis for populations of unicellular organisms (*Saccharomyces cerevisiae*). *Mech. Ageing Dev.* **38:**231–243; 1987.
[19] Muller, I. Parental age and the life-span of zygotes of *Saccharomyces cerevisiae*. *Antonie Leeuwenhoek* **51:**1–10; 1985.
[20] Muller, I.; Zimmermann, M.; Becker, D.; Flomer, M. Calendar life span versus budding life span of *Saccharomyces cerevisiae*. *Mech. Ageing Dev.* **12:**47–52; 1980.
[21] Tissenbaum, H. A.; Guarente, L. Model organisms as a guide to mammalian aging. *Dev. Cell* **2:**9–19; 2002.
[22] Johnson, F. B.; Sinclair, D. A.; Guarente, L. Molecular biology of aging. *Cell* **96:** 291–302; 1999.
[23] Motizuki, M.; Tsurugi, K. The effect of aging on protein synthesis in the yeast *Saccharomyces cerevisiae*. *Mech. Ageing Dev.* **64:**235–245; 1992.
[24] Pichova, A.; Vondrakova, D.; Breitenbach, M. Mutants in the *Saccharomyces cerevisiae RAS2* gene influence life span, cytoskeleton, and regulation of mitosis. *Can. J. Microbiol.* **43:**774–781; 1997.
[25] Serrano, M.; Lin, A. W.; McCurrach, M. E.; Beach, D.; Lowe, S. W. Oncogenic ras provokes premature cell senescence associated with accumulation of p53 and p16INK4a. *Cell* **88:**593–602; 1997.
[26] Sinclair, D. A.; Mills, K.; Guarente, L. Accelerated aging and nucleolar fragmentation in yeast *sgs1* mutants. *Science* **277:**1313–1316; 1997.
[27] Ghosh, H. S. The anti-aging, metabolism potential of SIRT1. *Curr. Opin. Investig. Drugs* **9:**1095–1102; 2008.
[28] Guarente, L. Sirtuins in aging and disease. *Cold Spring Harb. Symp. Quant. Biol.* **72:** 483–488; 2007.
[29] Laun, P.; Pichova, A.; Madeo, F.; Fuchs, J.; Ellinger, A.; Kohlwein, S.; Dawes, I.; Frohlich, K. U.; Breitenbach, M. Aged mother cells of *Saccharomyces cerevisiae* show markers of oxidative stress and apoptosis. *Mol. Microbiol.* **39:**1166–1173; 2001.
[30] Erjavec, N.; Nystrom, T. Sir2p-dependent protein segregation gives rise to a superior reactive oxygen species management in the progeny of *Saccharomyces cerevisiae*. *Proc. Natl Acad. Sci. USA* **104:**10877–10881; 2007.
[31] Drakulic, T.; Temple, M. D.; Guido, R.; Jarolim, S.; Breitenbach, M.; Attfield, P. V.; Dawes, I. W. Involvement of oxidative stress response genes in redox homeostasis, the level of reactive oxygen species, and ageing in *Saccharomyces cerevisiae*. *FEMS Yeast Res.* **5:**1215–1228; 2005.
[32] Aguilaniu, H.; Gustafsson, L.; Rigoulet, M.; Nystrom, T. Asymmetric inheritance of oxidatively damaged proteins during cytokinesis. *Science* **299:**1751–1753; 2003.
[33] Alic, N.; Felder, T.; Temple, M. D.; Gloeckner, C.; Higgins, V. J.; Briza, P.; Dawes, I. W. Genome-wide transcriptional responses to a lipid hydroperoxide: adaptation occurs without induction of oxidant defenses. *Free Radic. Biol. Med.* **37:**23–35; 2004.

[34] Klinger, H.; Rinnerthaler, M.; Lam, Y. T.; Laun, P.; Heeren, G.; Klocker, A.; Simon-Nobbe, B.; Dickinson, J. R.; Dawes, I. W.; Breitenbach, M. Quantitation of (a)symmetric inheritance of functional and of oxidatively damaged mitochondrial aconitase in the cell division of old yeast mother cells. *Exp. Gerontol.* **45:**533–542; 2010.
[35] Park, P. U.; McVey, M.; Guarente, L. Separation of mother and daughter cells. *Meth. Enzymol.* **351:**468–477; 2002.
[36] Mortimer, R. K.; Johnston, J. R. Life span of individual yeast cells. *Nature* **183:** 1751–1752; 1959.
[37] Egilmez, N. K.; Chen, J. B.; Jazwinski, S. M. Preparation and partial characterization of old yeast cells. *J. Gerontol.* **45:**B9–B17; 1990.
[38] Smeal, T.; Claus, J.; Kennedy, B.; Cole, F.; Guarente, L. Loss of transcriptional silencing causes sterility in old mother cells of S. cerevisiae. *Cell* **84:**633–642; 1996.
[39] Horisberger, M.; Rosset, J. Localization of wheat germ agglutinin receptor sites on yeast cells by scanning electron microscopy. *Experientia* **32:**998–1000; 1976.
[40] Lai, C. Y.; Jaruga, E.; Borghouts, C.; Jazwinskin, S. M. A mutation in the *ATP2* gene abrogates the age asymmetry between mother and daughter cells of the yeast *Saccharomyces cerevisiae*. *Genetics* **162:**73–87; 2002.
[41] Neklesa, T. K.; Davis, R. W. Superoxide anions regulate TORC1 and its ability to bind Fpr1:rapamycin complex. *Proc. Natl Acad. Sci. USA* **105:**15166–15171; 2008.
[42] Park, J. I.; Grant, C. M.; Davies, M. J.; Dawes, I. W. The cytoplasmic Cu, Zn superoxide dismutase of Saccharomyces cerevisiae is required for resistance to freeze–thaw stress: generation of free radicals during freezing and thawing. *J. Biol. Chem.* **273:**22921–22928; 1998.
[43] Breitenbach, M.; Laun, P.; Heeren, G.; Jarolim, S.; Pichova, A. Mother cells specific-ageing. In: Dickinson, J.R., Schweizer, M. (Eds.), The Metabolism and Molecular Physiology of Saccharomyces cerevisiae. CRC Press, Boca Raton, FL,pp. 20–41; 2004.
[44] Kirchman, P. A.; Botta, G. Copper supplementation increases yeast lifespan under conditions requiring respiratory metabolism. *Mech. Ageing Dev.* **128:**187–195; 2007.
[45] Grzelak, A.; Skierski, J.; Bartosz, G. Decreased antioxidant defense during replicative aging of the yeast *Saccharomyces cerevisiae* studied using the 'baby machine' method. *FEBS Lett.* **492:**123–126; 2001.
[46] Murray, D. B.; Beckmann, M.; Kitano, H. Regulation of yeast oscillatory dynamics. *Proc. Natl Acad. Sci. USA* **104:**2241–2246; 2007.
[47] Afanas'ev, I. B. Signaling functions of free radicals superoxide & nitric oxide under physiological & pathological conditions. *Mol. Biotechnol.* **37:**2–4; 2007.
[48] McCord, J. M.; Fridovich, I. Superoxide dismutase: an enzymic function for erythrocuprein (hemocuprein). *J. Biol. Chem.* **244:**6049–6055; 1969.
[49] Fridovich, I. Superoxide dismutases. *Annu. Rev. Biochem.* **44:**147–159; 1975.
[50] Erjavec, N.; Larsson, L.; Grantham, J.; Nystrom, T. Accelerated aging and failure to segregate damaged proteins in Sir2 mutants can be suppressed by overproducing the protein aggregation–remodeling factor Hsp104p. *Genes Dev.* **21:**2410–2421; 2007.